

Limits on the Mass of ν_τ from CLEO

Jean E. Duboscq

^aDepartment of Physics, The Ohio State University, Columbus, OH 43210-1168 USA
email: jed@mail.lns.cornell.edu

A limit on the mass of the tau neutrino m_{ν_τ} is derived from 4.5×10^6 tau pairs produced in an integrated luminosity of 5.0 fb^{-1} of $e^+e^- \rightarrow \gamma^* \rightarrow \tau^+\tau^-$ reactions at center of mass energies $\approx 10.6 \text{ GeV}$. The measurement technique involves a two-dimensional extended likelihood analysis, including the dependence of the end-point population on m_{ν_τ} , and allows for the first time an explicit background contribution. We use the decays $\tau \rightarrow 5\pi\nu_\tau$ and $\tau \rightarrow 3\pi 2\pi^0\nu_\tau$ to obtain an upper limit of $30 \text{ MeV}/c^2$ at 95% C.L., as well as a preliminary limit of $31 \text{ MeV}/c^2$ from $\tau \rightarrow 3\pi\pi^0\nu_\tau$.

1. Introduction

We present two separate analyses of the mass of the ν_τ . The first analysis, as published in [1], herein referred to as the $5h$ analysis, comprises a sample of the decays $\tau \rightarrow 5\pi\nu_\tau$ and $\tau \rightarrow 3\pi 2\pi^0\nu_\tau$. These decay modes have a small overall branching fraction but a significant probability of populating the hadronic mass end-point sensitive to m_ν . The second (preliminary) analysis, herein referred to as the $4h$ analysis, exploits the decay $\tau \rightarrow 3\pi\pi^0\nu_\tau$. Although the probability per event of being near the endpoint is much smaller in this sample, the much larger branching ratio makes it competitive.

2. The CLEO Analysis Method

The analyses use the two-dimensional hadronic energy versus hadronic mass spectrum, first used in [2], to obtain a limit on the mass of the ν_τ . The selection criteria require well reconstructed tracks, as well as good quality π^0 candidates, when appropriate, recoiling against a well separated one prong tag. For the $5h$ analysis, the tag track is required to be an identified lepton, while in the $4h$ analysis, the tag must be consistent with either an electron, muon, π or ρ . Stringent excess energy criteria reduce the possible backgrounds in both analyses. In the $5h$ analysis only a small region near the endpoint is used for the fit. For that

analysis, an extra Poisson coefficient is used in an extended likelihood, relating the number of events expected in the Fit Region at the endpoint as a function of neutrino mass to the number of events observed in data in a neutrino-mass-insensitive Control Region (see Fig 1.) The fit region for the $4h$ analysis is chosen large enough to make the Poisson term unnecessary. For the first time in any ν_τ mass analysis, both the $5h$ and $4h$ fits allow for an explicit background term to account for non-signal events.

3. The $5h$ Sample

The final event sample is summarized in Table 1. The hadronic masses of the $5h$ samples are displayed in Fig 2. There are 207 events in the $3\pi 2\pi^0$ sample and 266 events in the 5π sample. Backgrounds can come from either misreconstructed tau decays or from non-tau sources such as charm decays. The non-tau background estimator shape used in the fit is obtained from a data sample of events with tracks in one hemisphere with loose selection criteria and invariant mass above the tau mass recoiling against either 5π or $3\pi 2\pi^0$ candidates. Its normalization is provided by the number of events in Fig 2 above the tau mass¹. Backgrounds from tau decays to fi-

¹ Corrections for τ event feed-across into the background estimator are negligible.

Table 1
Summary of $5h$ and $4h$ analyses

Mode	5π	$3\pi 2\pi^0$	$4h$
Total events	266	207	29×10^3
Events in Fit Region	36	19	17×10^3
Fit Region Purity (%)	99	93	90
Selection Efficiency (%)	3.1	0.4	2.6
Typical Mass Resolution (MeV/c^2)	15	25	20
Typical Energy Resolution (MeV)	25	50	38
Uncorrected Upper Limit @ 95 % CL (MeV/c^2)	31	33	26

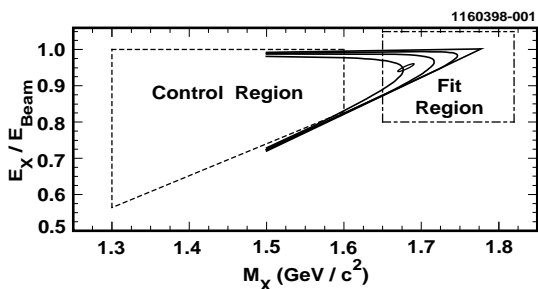


Figure 1. The number of events in the the Fit Region relative to the number in the Control Region in the scaled hadronic energy versus hadronic mass plane is a function of neutrino mass. Kinematically allowed neutrino mass contours are drawn for neutrino masses of 0, 30, 60 and $100 \text{ MeV}/c^2$. Note the typical error ellipse drawn in the fit region.

nal states other than 5π and $3\pi 2\pi^0$ are estimated from Monte Carlo studies², and are expected to be small. The hadronic energy scaled to beam energy versus hadronic mass distribution is shown in Fig 3 for events in the neutrino mass sensitive Fit Region.

4. The $4h$ Sample

The scaled energy versus mass distribution of the full sample of $4h$ decays is shown in Fig 4. As noted in table 1, there about 29K events in the sample, with 17K events in the fit region. In

² The CLEO Monte Carlo is based on [3-6].

addition to the dominant $3\pi\pi^0$ final state, the data sample includes other $3h\pi^0$ resulting from the $K_s\pi\pi^0$, $K\omega$, $KK_s\pi^0$ and $\pi\omega\pi^0$ intermediate hadronic states. All these are included in the fit. The backgrounds are predominantly from misreconstructed tau events in the Fit Region (7%) and decays of $q\bar{q}$ pairs (3%). These background shapes are estimated from Monte Carlo. The tau background sample normalization is estimated from Monte Carlo, and the $q\bar{q}$ background normalized to the number of events seen in the data above the tau mass, corrected for τ feedthroughs.

5. Spectral Functions

The invariant mass spectra used in the $5h$ analysis are fit in an independent data sample of π tagged $5h$ decays. The fit functions are derived from that expected from $e^+e^- \rightarrow 4\pi$ distributions, along with soft pion theorems, as well as the shape expected for $\tau \rightarrow 6\pi\nu$, as extrapolated from $e^+e^- \rightarrow 6\pi$ distributions [8-10]. The former shape is expected to dominate, while the latter shape is allowed in the fit as a purely phenomenological tuning parameter. Since the 6π shape expects events at higher masses than the 4π shape, its inclusion naturally leads to a more conservative limit. The fit also includes a background shape, and excludes the mass range within $100 \text{ MeV}/c^2$ of the tau mass to decrease bias on the neutrino mass. The final distributions are shown in Fig 5. The $4h$ spectral function is dominated by the $3\pi\pi^0$ final state. This state arises via intermediate decays including a ρ , ρ' , ρ'' or an ω . The spectral function is obtained by the

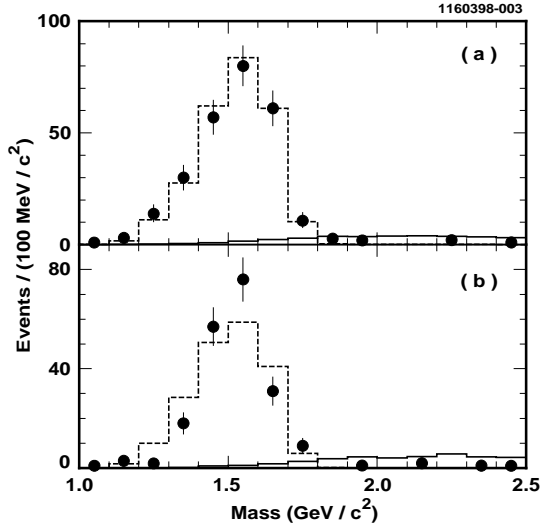


Figure 2. The hadronic mass for the 5π (a) and $3\pi 2\pi^0$ (b) event candidates. The Monte Carlo estimation of signal shape, normalized to the data sample size in the control region, is displayed as the dotted histogram. The solid histogram is the background estimator displayed at five times its true size for illustration purposes.

fitting all 2π , 3π and 4π combinations in the current to a sum of such intermediate states, as an extension of the model used in Tauola[5]:

$$J = F^{\rho\pi\pi}(Q_{4\pi}^2)\sum_{i=1,5}\mathcal{A}_i f_i^\rho(q_{2i}) + F^{\omega\pi}(Q_{4\pi}^2)\sum_{i=1,2}\mathcal{A}_i f_i^\omega(q_{3i})$$

where $F^{\rho\pi\pi}$, $F^{\omega\pi}$, and f^ρ are sums of Breit-Wigner distributions for the ρ , ρ' and ρ'' , and f^ω is a Breit-Wigner distribution for the ω . The 4π combinations used are only those with a mass below $1.6 \text{ GeV}/c^2$. Other $3h\pi^0$ decays modes not considered in the above are small and fixed to their Monte Carlo expected shapes. Although this is not a unique model for this decay, all mass distribution projections fit very well - see Fig 6.

6. The Likelihood Functions

The event likelihood includes both a signal shape with a dependence on neutrino mass, and

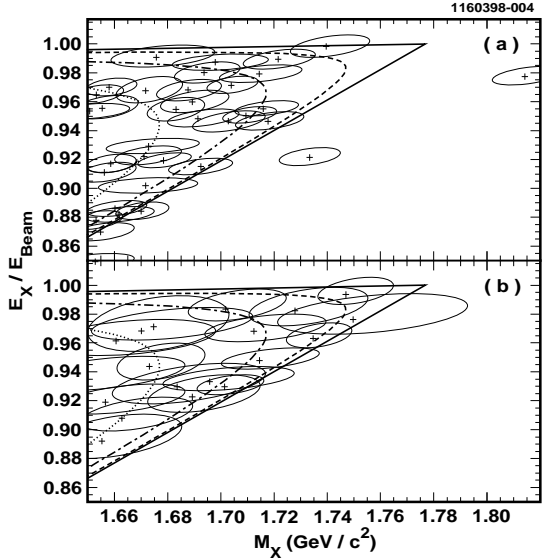


Figure 3. The hadronic energy (scaled to beam energy) vs hadronic mass for (a) the 5π and the (b) $3\pi 2\pi^0$ event candidates in the fit region. Ellipses represent 68% confidence levels.

a background shape:

$$\mathcal{L}_{event}(M_\nu) = \alpha \mathcal{L}_{sig}(data, M_\nu) + (1 - \alpha) \mathcal{L}_{bgd}(data)$$

where α sets the relative background and signal sizes³. The full likelihood is a product over the individual event likelihoods, and, for the $5h$ analysis, includes a Poisson coefficient $P(N_{obs}, M_\nu)$ to account for the expected number of events in the Fit Region given the number of events in the Control Region, and the neutrino mass.

The signal likelihood used in previous analyses [7] relied on convolutions of parametrizations of Monte Carlo data. The present analyses forego the unnecessary convolution and parametrisation steps, and fit directly to Monte Carlo data. Re-

³ Note that an a priori assumption on the neutrino mass allowed range must be made for normalization purposes. In this case we chose to assume that $M_\nu < 100 \text{ MeV}/c^2$. The result is not strongly dependent on this assumption for reasonable a priori distributions.

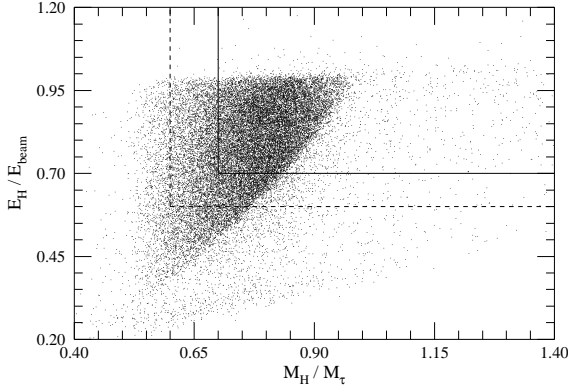


Figure 4. The hadronic energy (scaled to beam energy) vs hadronic mass (scaled to τ mass) for the $4h$ sample. The solid lines indicate the Fit Region, while the dashed line indicates a larger fit region used in systematics studies.

constructed Monte Carlo events, generated with a massless neutrino, are accepted or rejected by the data selection criteria. Their generated mass and energy are then smeared according to an analytic detector smearing function, depending only on hadronic mass and energy, and their associated propagated tracking and calorimetry errors. Furthermore, this smearing function is taken as universal for all events in the same sample when scaled according to propagated mass and energy errors. The probability that a Monte Carlo event could be reconstructed as the data event in question is proportional to the smearing. Symbolically,

$$\mathcal{L}_{sig} \propto \sum_{MC} G\left(\frac{\tilde{X}_{data} - X_{MC}}{\sigma}\right) \mathcal{W}(X_{MC}, M_\nu) \quad (1)$$

where G represents the detector smearing function, and \mathcal{W} is an exactly calculable weight factor for neutrino mass hypotheses relative to a massless neutrino. The smearing function is obtained from Monte Carlo τ decays and is parametrised as the sum of three 2 dimensional Gaussians.

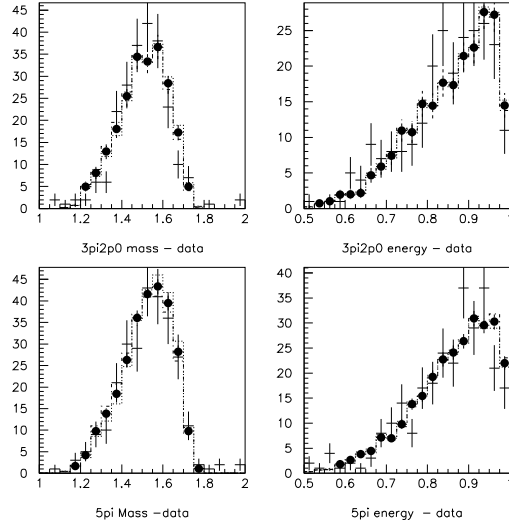


Figure 5. The fitted spectral functions compared to the data for the $5h$ samples. The top (bottom) plots show the $3\pi 2\pi^0$ (5π) sample mass fit and resulting energy projections. The crosses represent the $5h$ data, while the dots represent the fit, while the estimated errors in the fit are shown by the histograms. Note that the fit was performed on a statistically independent sample.

7. Results

The final likelihoods are shown in Fig 7 and Fig 8. An integral of the likelihood from 0 MeV/c^2 to 95% of the full area of the likelihood gives raw upper limits of 33, 31 and 26 MeV/c^2 respectively for the $3\pi 2\pi^0$, 5π and $4h$ samples. Combining the $3\pi 2\pi^0$ and 5π likelihoods give a raw upper limit of 27 MeV/c^2 . Including the $4h$ likelihood lowers the uncorrected upper limit to 25 MeV/c^2 . Systematic errors were carefully examined for the combined $5h$ studies and the $4h$ study. Charm meson decays to $K\pi$, $K2\pi$ and $K3\pi$ final states in data and Monte Carlo show good agreement for the smearing functions, and are used to estimate systematic errors for the smearing function along the mass axis. Since B mesons at CLEO are produced at rest, the mass

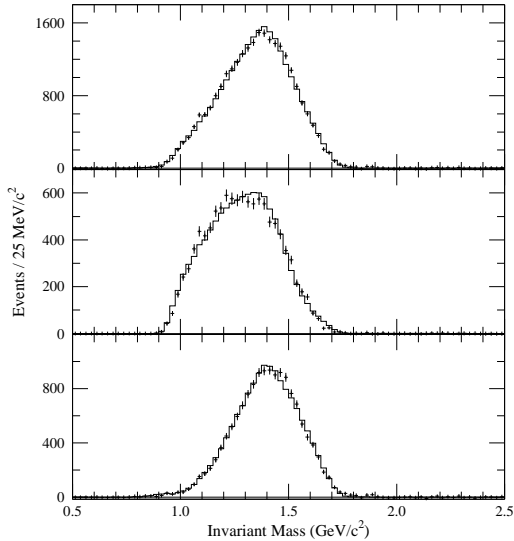


Figure 6. The spectral function used in the $4h$ sample fit, for events containing no ω (top), those containing an ω (middle), and all events (bottom).

spectra of hadronic final states of B meson decays give a direct measure of the smearing along the energy axis. Smearing modeling systematics contribute 1.5 and 0.4 MeV/c^2 to the $5h$ and $4h$ studies respectively. The spectral functions are all allowed to vary according to the uncertainties in their associated fits, contributing 1.9 and 1.2 MeV/c^2 respectively. The CLEO mass and momentum reconstruction scales are also considered as sources of error (1.5 and 2.3 MeV/c^2 respectively) as was the CLEO energy scale (0.2 and 3.7 MeV/c^2)⁴ The sum in quadrature of all considered systematic errors is 3.1 MeV/c^2 for the $5h$ study and 5.1 MeV/c^2 for the $4h$ study. Following the conservative prescription used by the LEP experiments [7], these errors are added lin-

⁴ Differences in nomenclature for systematic errors between the studies explain the apparent size inconsistencies of systematic errors. For instance, modeling of the π^0 contribution in the smearing is accounted for as a smearing systematic in the $5h$ study, and as a momentum scale systematic error in the $4h$ study.

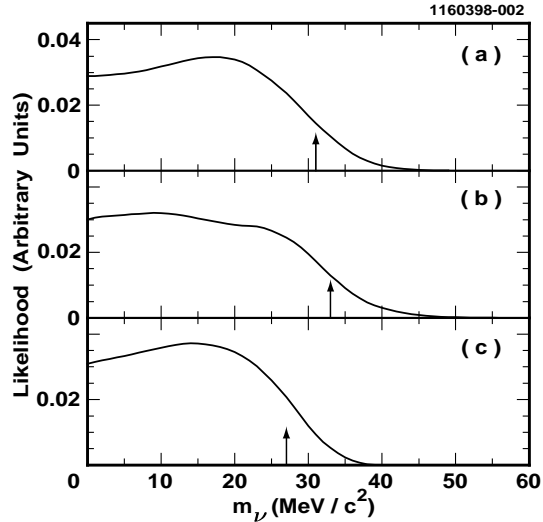


Figure 7. The likelihood function versus neutrino mass from the $5h$ sample fit for the $3\pi 2\pi^0$ sample (top), 5π sample (middle) and the combined $5h$ sample (bottom).

M_ν^{in} MeV/c^2	25 events	450 events
0	3%	67%
50	$\approx 1\%$	$< 1\%$

Table 2

Probability of a 95th percentile below 27 MeV/c^2 for small and large data samples given a true neutrino mass of 0 and 50 MeV/c^2 .

early to the upper limits, resulting in an upper limit of 30 MeV/c^2 for the $5h$ sample and a preliminary limit of 31 MeV/c^2 for the $4h$ sample, all at the 95% confidence level. The combination of the $5h$ and $4h$ studies is still under consideration at this writing. The interpretation of the 95th percentile of a likelihood as a statement of probability about the neutrino mass is dependent upon the experimentally reconstructed likelihood being representative of an ensemble of likelihoods for samples drawn from a distribution with similar properties. Thus conclusions drawn from exper-

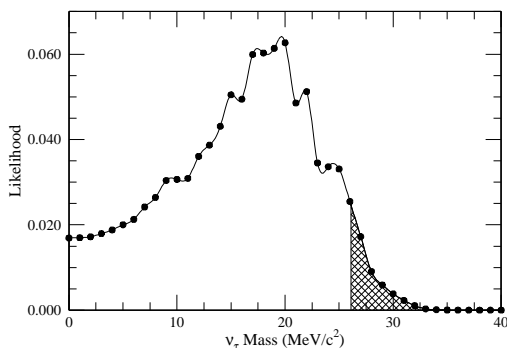


Figure 8. The likelihood function versus neutrino mass from the $4h$ sample fit. The small bin to bin variations result from limited Monte Carlo statistics, and are not significant.

iments with small statistics must be interpreted with care especially when very stringent limits are quoted. These limits tend to have much lower discriminatory power than one might naively think. Table 2 illustrates this for studies done with the CLEO Monte Carlo. For a sample of 25 events, a 95th percentile limit of $27 \text{ MeV}/c^2$ is obtainable 3% of the time with a massless neutrino but it is also obtainable about 1% of the time with a $50 \text{ MeV}/c^2$ neutrino. The discriminatory power is of course much better for larger samples. Extensive Monte Carlo studies have shown that the 95th percentile upper limits obtained for the $5h$ samples in this study are not unlikely - in some 35 % (74 %) of Monte Carlo experiments with similar statistics, the 95th percentile was found to be larger than that found in the data for the 5π ($3\pi 2\pi^0$) sample. Thus the interpretation of the combined 95th percentile as an upper limit is credible.

In all the fits presented here, the likelihood peaks away from $0 \text{ MeV}/c^2$. In no case however is the peaking deemed to be significant. In the $4h$ study, the ratio of likelihoods at the peak relative to that at $0 \text{ MeV}/c^2$ corresponds to a 1.6σ effect if one assumes that the underlying probability densities are Gaussian. Multiple Monte Carlo experiments, as well as basic statistical the-

ory, also show that the likelihood function is not always expected to peak at $0 \text{ MeV}/c^2$, even for a truly massless neutrino. In addition the conservative approximations made in the analysis can not only result in less stringent limits, but can also have the effect of pushing any peak further from $0 \text{ MeV}/c^2$. These likelihood curves should not therefore be used to infer the existence of a massive neutrino.

8. Conclusions

Using the world's largest dataset, CLEO sets a combined upper limit of $30 \text{ MeV}/c^2$ for a combined study of $\tau \rightarrow 5\pi\nu$, $\tau \rightarrow 3\pi 2\pi^0\nu$ decays and a preliminary upper limit of $31 \text{ MeV}/c^2$ from the decay $\tau \rightarrow 3h\nu$. These limits use a novel Monte Carlo integration technique, and are the first to explicitly account for possible backgrounds in the likelihood function.

REFERENCES

1. CLEO Coll., R. Ammar *et al*, Phys. Lett. B 431 (1998) 209
2. OPAL Collab., R. Akers *et al*, Z. Phys. C 65 (1995) 183
3. S.J. Sojstrand, LUND 7.3, CERN-TH-6488-92 (1992)
4. R. Brun *et al.*, GEANT v. 3.14, CERN Report No. CC/EE/84-1 (1987)
5. KORALB (v2.2)/TAUOLA (V2.4): S. Jadach and Z. Was, Comp. Phys. Com. 36 (1985) 191 and *ibid* 64 (1991) 267; S. Jadach, J.H. Kühn and Z. Was, Comp. Phys. Com. 64 (1991) 275, *ibid*, 70 (1992) 69, and *ibid*, 76 (1993) 361
6. E. Barbiero, B. van Eijk and Z. Was, CERN-TH-5857/90 (1990)
7. L. Passalacqua, Nucl. Phys. B (Proc. Sup.) 55 (1996) 435
8. Y.S. Tsai, Phys. Rev. D 4 (1971) 2821
9. F. Gilman and D. Miller, Phys. Rev. D 17 (1978) 1846
10. T.N. Pham, C. Roiesnel and T.N. Truong, Phys. Lett. B 78 (1978) 623